Supporting Information

Kinetic Modeling Study of the Group-Transfer Polymerization of Alkyl Crotonates Using a Silicon Lewis Acid Catalyst

Table of Contents

Figure S1. ^{13}C NMR spectra of poly(MC) and poly(EC) synthesized at 20 °C.

Figure S2. Curve fittings for the GTP of EC using Tf_2NSiEt_3/^{Et3}SKA at T_r.

Figure S3. Curve fittings for the GTP of EC using $Tf_2NSi^tBuMe_2$/^{tBuMe2}SKA at T_r.

Figure S4. Curve fittings for the GTP of EC using $Tf_2NSi^iPr_3$/^{iPr3}SKA at T_r.

Figure S5. Curve fittings for the GTP of EC using Tf_2NSiEt_3/^{Et3}SKA at various temperatures.

Figure S6. Curve fittings for the GTP of EC using $Tf_2NSi^tBuMe_2$/^{tBuMe2}SKA at various temperatures.

Figure S7. Curve fittings for the GTP of EC using $Tf_2NSi^iPr_3$/^{iPr3}SKA at various temperatures.

Figure S8. ^{1}H NMR spectrum of ^{Et3}SKA in $CDCl_3$ at room temperature.

Figure S9. ^{1}H NMR spectrum of ^{tBuMe2}SKA in $CDCl_3$ at room temperature.

Figure S10. ^{1}H NMR spectrum of ^{iPr3}SKA in $CDCl_3$ at room temperature.

Scheme S1. Generation of a silicon LA catalyst in situ.

Table S1. Summarized data on the GTP of EC using silicon LA catalysts and SKAs having various trialkylsilyl moieties.

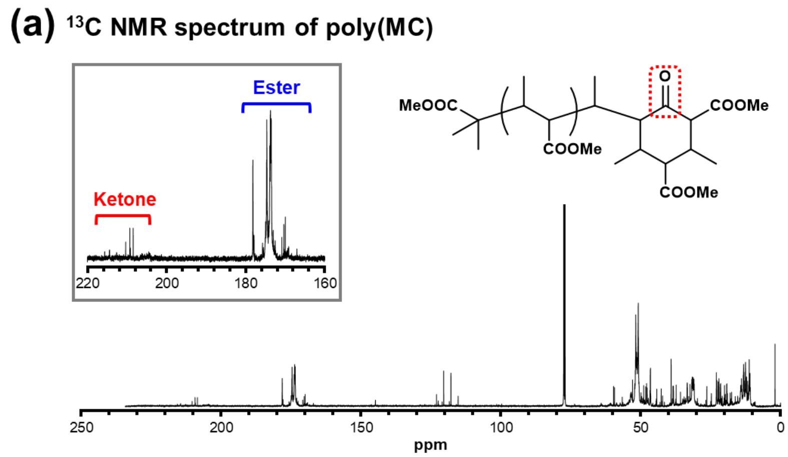

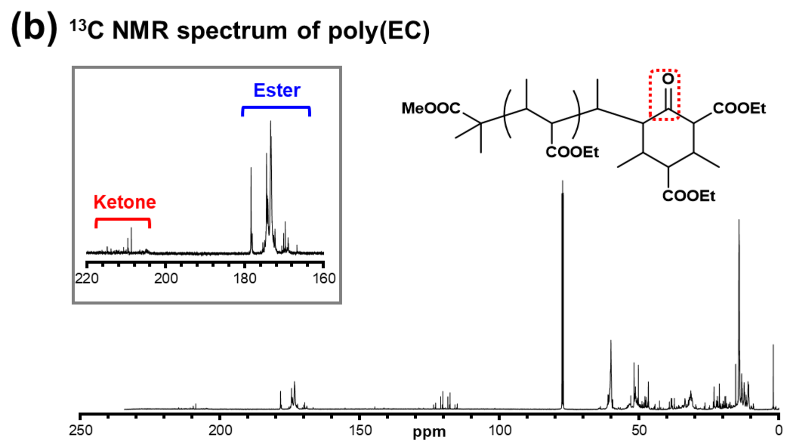

Figure S1. ^{13}C NMR spectra of **(a)** poly(MC) and **(b)** poly(EC) synthesized at 20 °C, measured in $CDCl_3$ at room temperature and 125 MHz.

(a) The polymer sample was synthesized by the reaction of MC (10 mmol) with MTS (1.0 mmol) and Tf_2NSiMe_3 (1.0 mmol) in CH_2Cl_2 (8.7 mL) at 20 °C for 24 h. The monomer conversion was 86.7%. Number-averaged molecular weight (M_n) and dispersity ($Đ$) were 1,100 g mol^{-1} and 1.61, respectively. The resonance peaks derived from ketone carbons were observed in the range of 205–220 ppm, in addition to the resonance peaks derived from ester carbons (165–180 ppm).

(b) The polymer sample was synthesized by the reaction of EC (10 mmol) with MTS (1.0 mmol) and Tf_2NSiMe_3 (1.0 mmol) in CH_2Cl_2 (8.6 mL) at 20 °C for 24 h. The monomer conversion was 95.2%. Number-averaged molecular weight (M_n) and dispersity ($Đ$) were 1,200 g mol^{-1} and 1.56, respectively. The resonance peaks derived from ketone carbons were observed in the range of 205–220 ppm, in addition to the resonance peaks derived from ester carbons (165–180 ppm).

These spectrometric results support the presence of cyclic structures generated through a cyclization reaction, and validity of this kinetic model asserting that main termination reaction is cyclization.

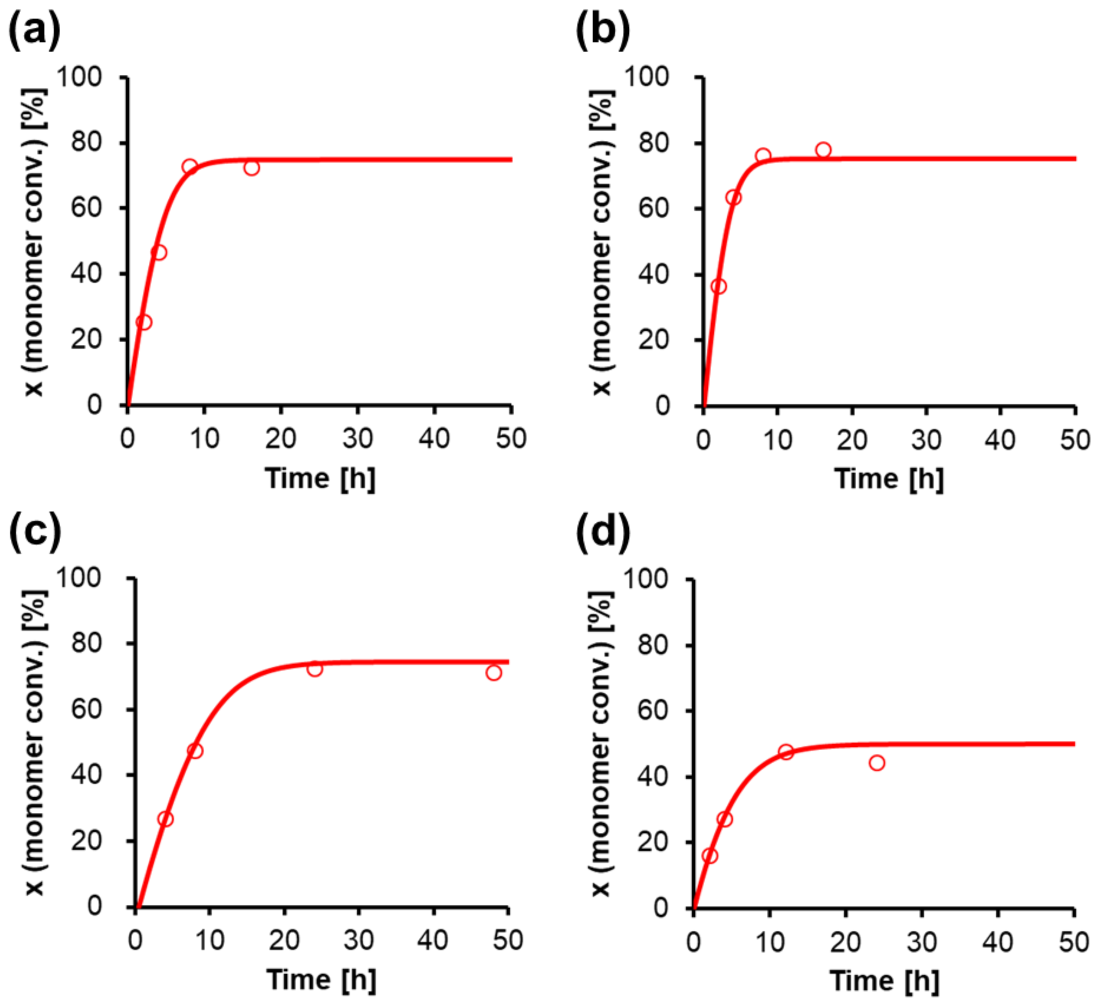

Conditions:

(a) $[EC]_0$ = 2.0 M, $[^{Et3}SKA]_0$ = 0.0050 M, $[Tf_2NSiEt_3]_0$ = 0.0050 M
(b) $[EC]_0$ = 1.5 M, $[^{Et3}SKA]_0$ = 0.0050 M, $[Tf_2NSiEt_3]_0$ = 0.0050 M
(c) $[EC]_0$ = 2.0 M, $[^{Et3}SKA]_0$ = 0.0050 M, $[Tf_2NSiEt_3]_0$ = 0.0025 M
(d) $[EC]_0$ = 1.0 M, $[^{Et3}SKA]_0$ = 0.0025 M, $[Tf_2NSiEt_3]_0$ = 0.0025 M

Figure S2. Curve fittings for the GTP of EC using $Tf_2NSiEt_3/^{Et3}SKA$ at T_r (10 °C). The symbols represent the experimental data, and the lines represent the simulation results. The experimental data correspond to **(a)** entries 1–4, **(b)** entries 5–8, **(c)** entries 9–12, and **(d)** entries 13–16 in **Table S1**.

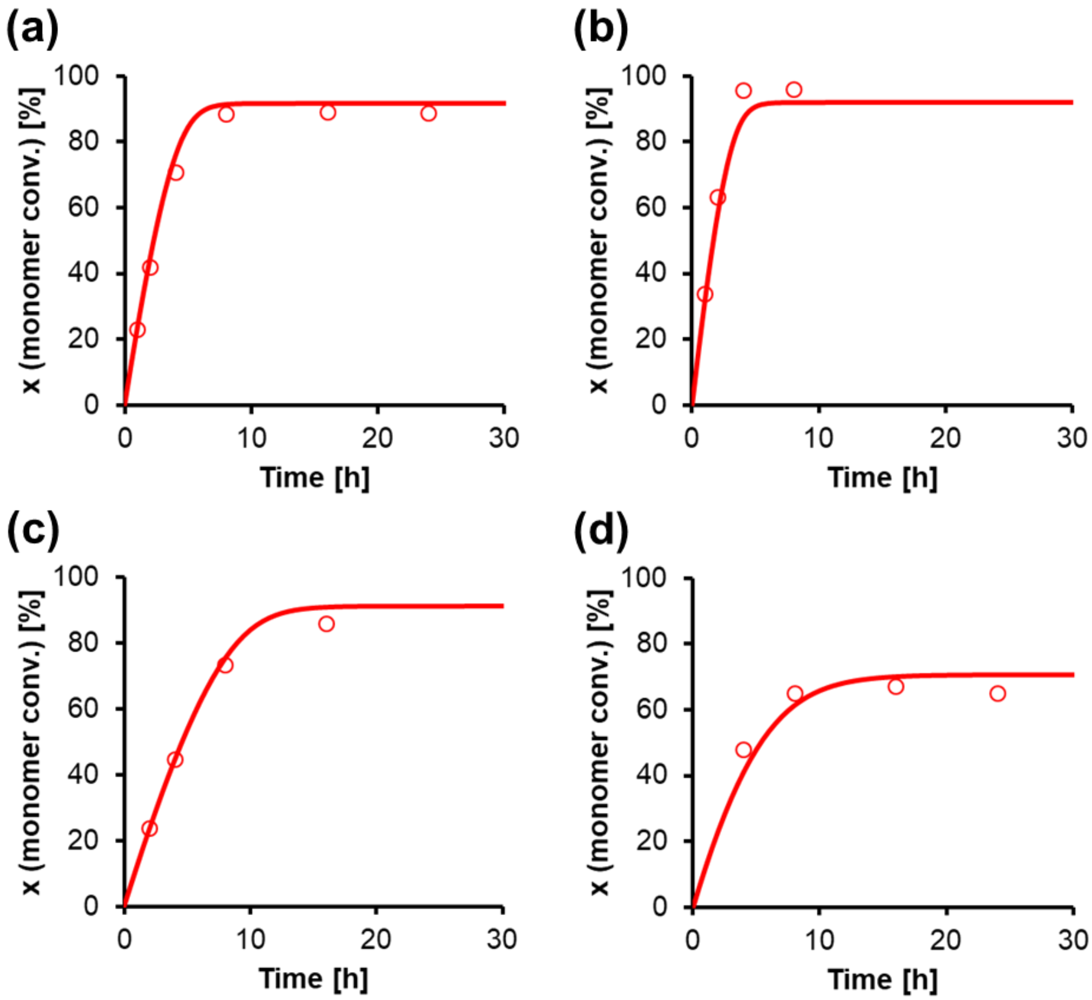

Conditions:

(a) $[EC]_0$ = 2.0 M, $[^{tBuMe2}SKA]_0$ = 0.0050 M, $[Tf_2NSi^tBuMe_2]_0$ = 0.0050 M

(b) $[EC]_0$ = 1.5 M, $[^{tBuMe2}SKA]_0$ = 0.0050 M, $[Tf_2NSi^tBuMe_2]_0$ = 0.0050 M

(c) $[EC]_0$ = 2.0 M, $[^{tBuMe2}SKA]_0$ = 0.0050 M, $[Tf_2NSi^tBuMe_2]_0$ = 0.0025 M

(d) $[EC]_0$ = 1.0 M, $[^{tBuMe2}SKA]_0$ = 0.0025 M, $[Tf_2NSi^tBuMe_2]_0$ = 0.0025 M

Figure S3. Curve fittings for the GTP of EC using $Tf_2NSi^tBuMe_2/^{tBuMe2}SKA$ at T_r (30 °C). The symbols represent the experimental data, and the lines represent the simulation results. The experimental data correspond to **(a)** entries 37–42, **(b)** entries 43–46, **(c)** entries 47–50, and **(d)** entries 51–54 in **Table S1**.

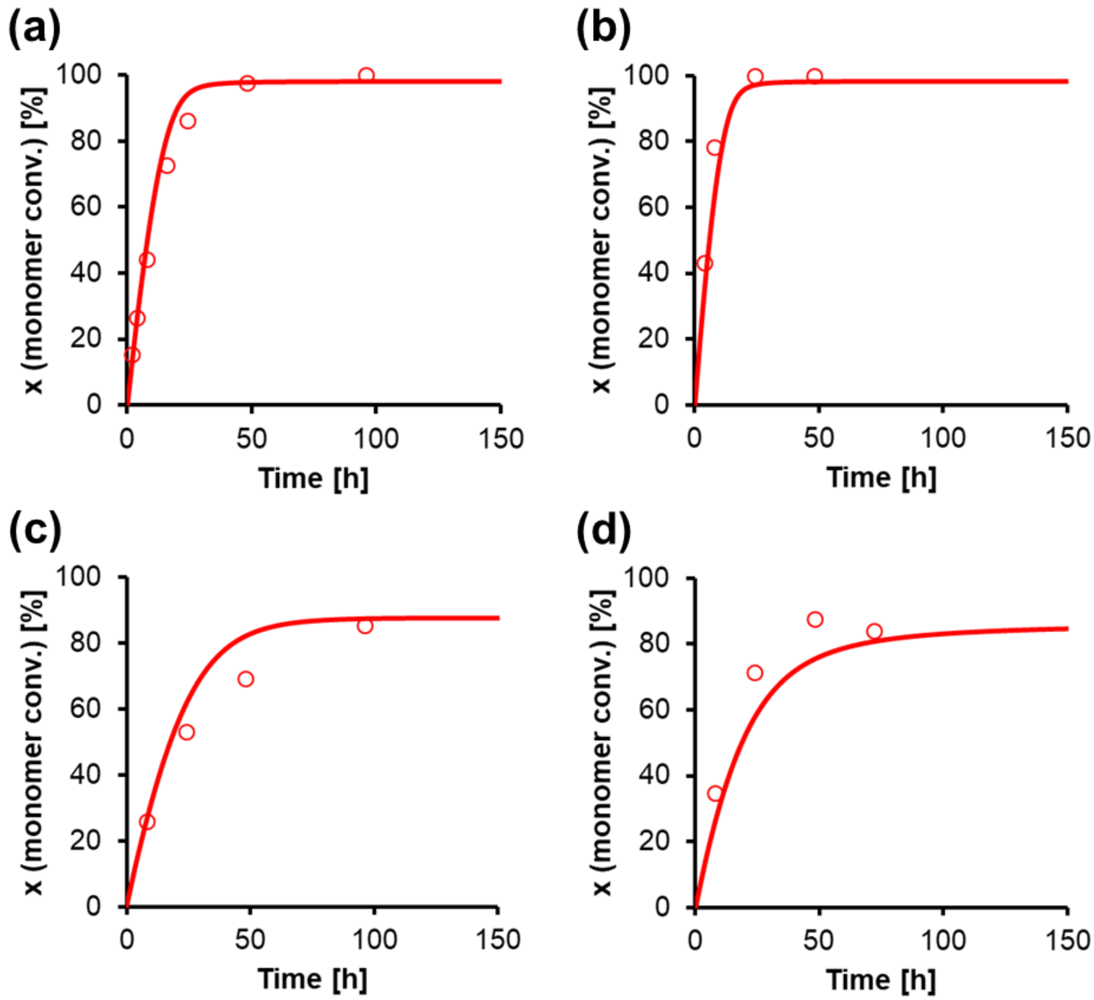

Conditions:
(a) $[EC]_0$ = 2.0 M, $[^{iPr3}SKA]_0$ = 0.0050 M, $[Tf_2NSi^iPr_3]_0$ = 0.0050 M
(b) $[EC]_0$ = 1.5 M, $[^{iPr3}SKA]_0$ = 0.0050 M, $[Tf_2NSi^iPr_3]_0$ = 0.0050 M
(c) $[EC]_0$ = 2.0 M, $[^{iPr3}SKA]_0$ = 0.0050 M, $[Tf_2NSi^iPr_3]_0$ = 0.0025 M
(d) $[EC]_0$ = 1.0 M, $[^{iPr3}SKA]_0$ = 0.0025 M, $[Tf_2NSi^iPr_3]_0$ = 0.0025 M

Figure S4. Curve fittings for the GTP of EC using $Tf_2NSi^iPr_3/^{iPr3}SKA$ at T_r (40 °C). The symbols represent the experimental data, and the lines represent the simulation results. The experimental data correspond to **(a)** entries 67–73, **(b)** entries 74–77, **(c)** entries 78–81, and **(d)** entries 82–85 in **Table S1**.

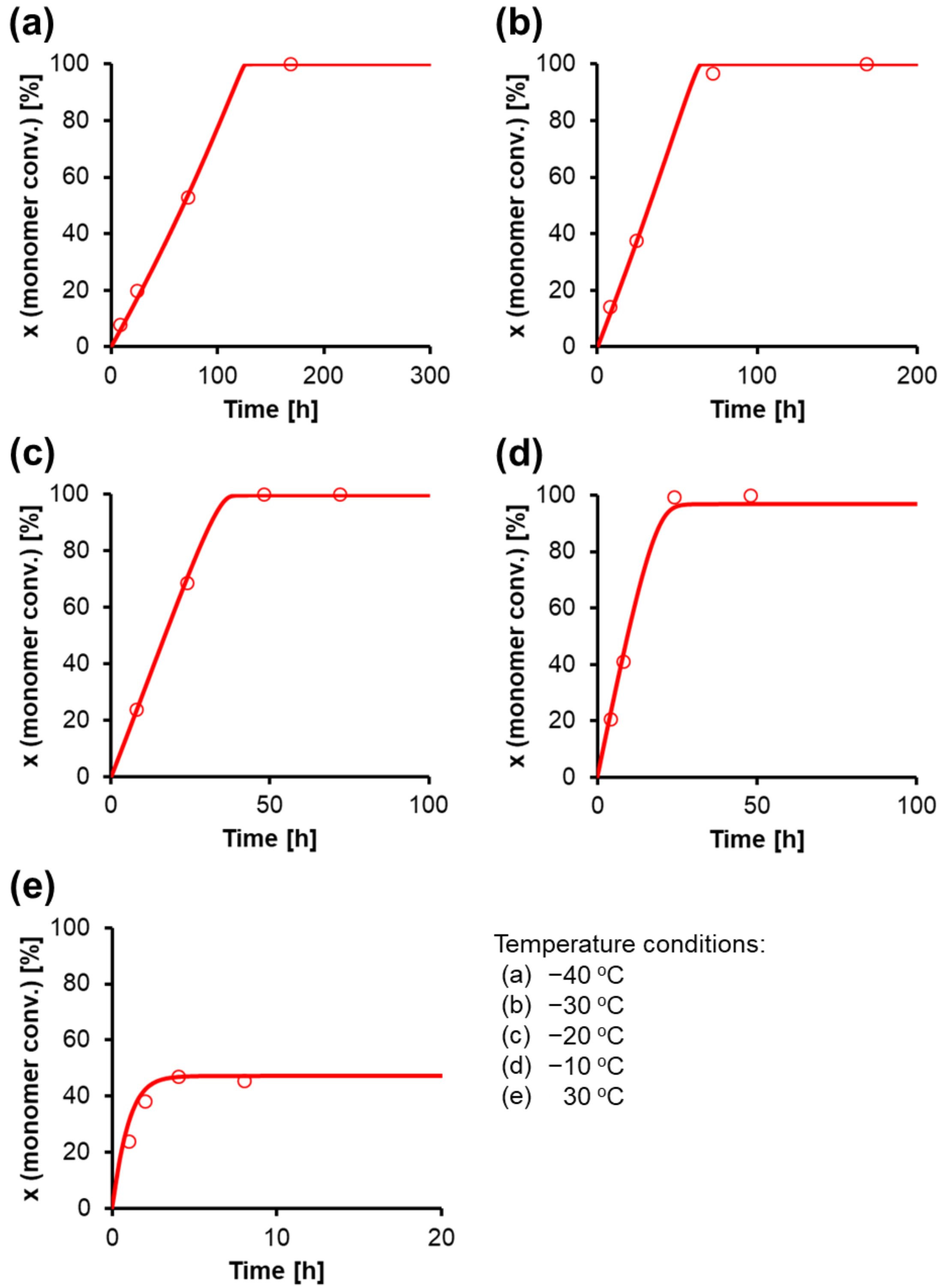

Figure S5. Curve fittings for the GTP of EC using $Tf_2NSiEt_3/^{Et3}SKA$ at various temperatures. The conditions are as follows: $[EC]_0 = 2.0$ M, $[^{Et3}SKA]_0 = 0.0050$ M, and $[Tf_2NSiEt_3]_0 = 0.0050$ M. The symbols represent the experimental data, and the lines represent the simulations. The experimental data correspond to **(a)** entries 17–20, **(b)** entries 21–24, **(c)** entries 25–28, **(d)** entries 29–32, and **(e)** entries 33–36 in **Table S1**.

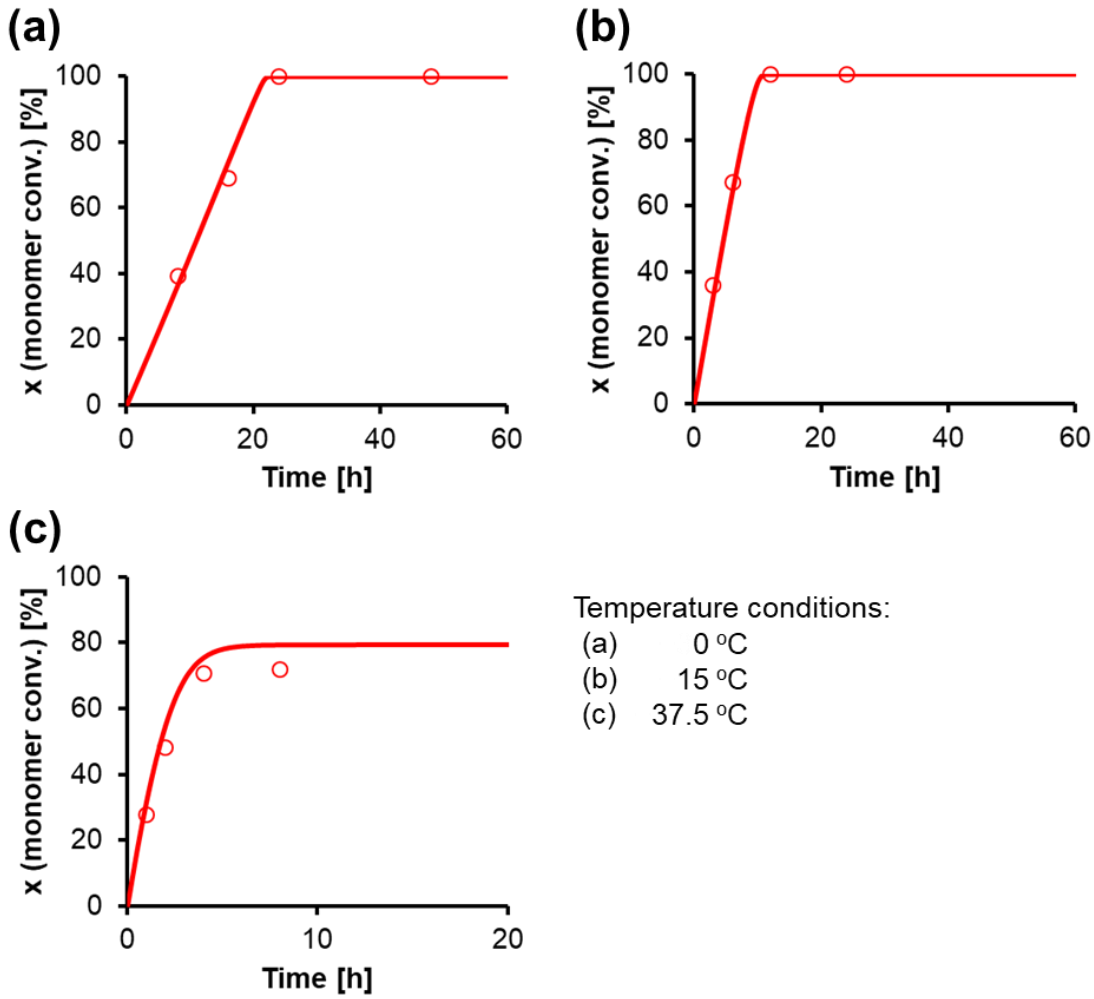

Figure S6. Curve fittings for the GTP of EC using $Tf_2NSi^tBuMe_2$/^{tBuMe2}SKA at various temperatures. The conditions are as follows: $[EC]_0$ = 2.0 M, $[^{tBuMe2}SKA]_0$ = 0.0050 M, and $[Tf_2NSi^tBuMe_2]_0$ = 0.0050 M. The symbols represent the experimental data, and the lines represent the simulation results. The experimental data correspond to **(a)** entries 55–58, **(b)** entries 59–62, and **(c)** entries 63–66 in **Table S1**.

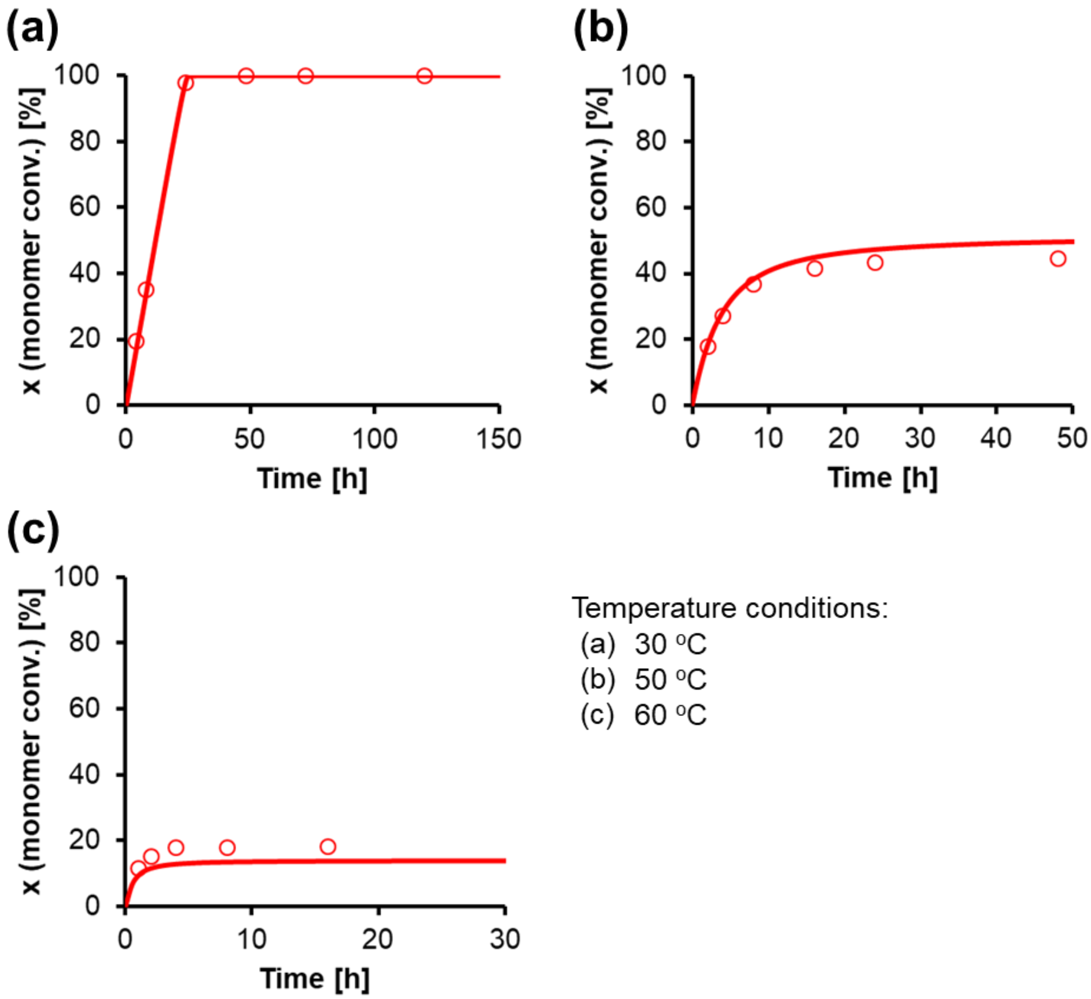

Figure S7. Curve fittings for the GTP of EC using $Tf_2NSi^iPr_3/^{iPr3}SKA$ at various temperatures. The conditions are as follows: $[EC]_0$ = 2.0M, $[^{iPr3}SKA]_0$ = 0.0050M, and $[Tf_2NSi^iPr_3]_0$ = 0.0050M. The symbols represent the experimental data, and the lines represent the simulation results. The experimental data correspond to **(a)** entries 86–91, **(b)** entries 92–97, and **(c)** entries 98–102 in **Table S1**.

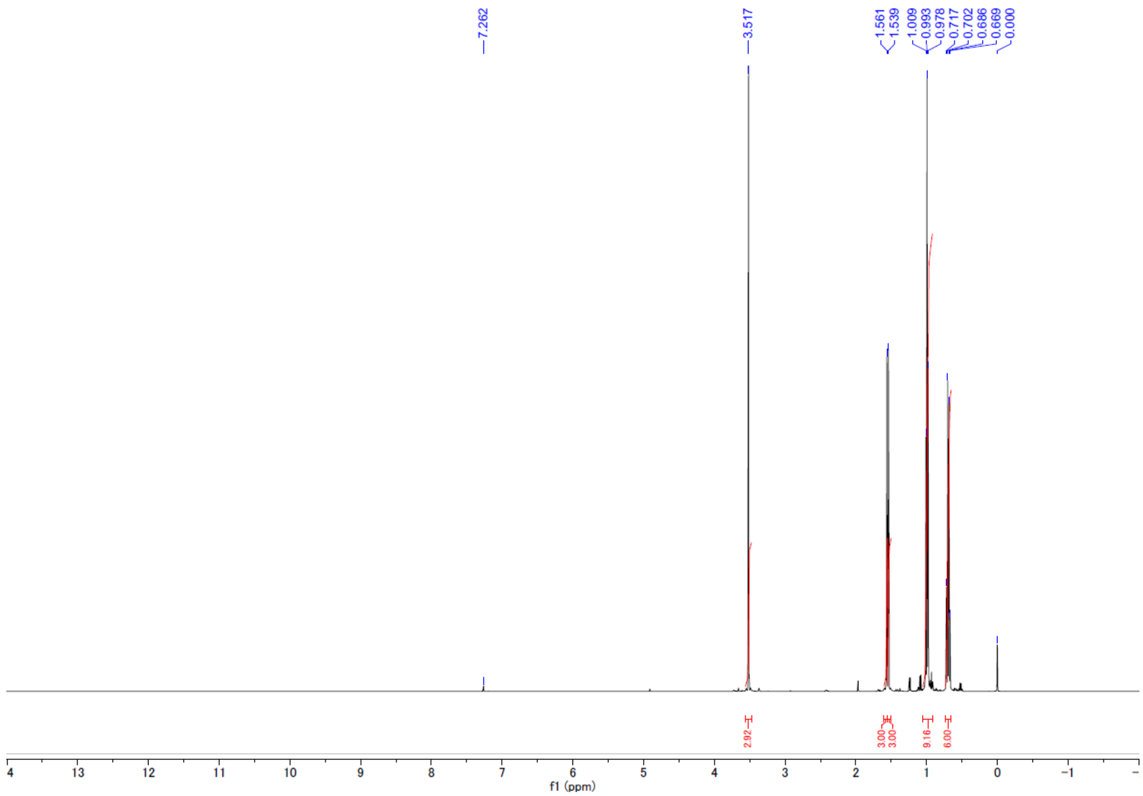

Figure S8. ^{1}H NMR spectrum of ^{Et3}SKA in $CDCl_3$ at room temperature.

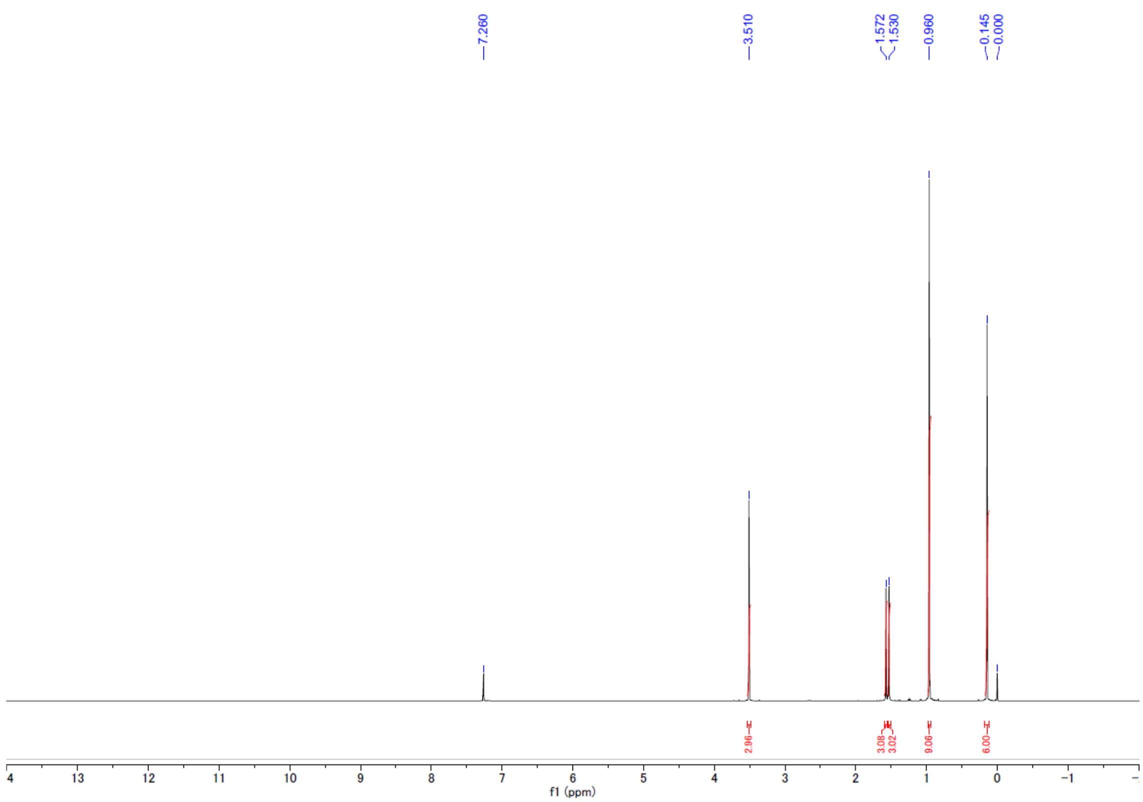

Figure S9. ^{1}H NMR spectrum of ^{tBuMe2}SKA in $CDCl_3$ at room temperature.

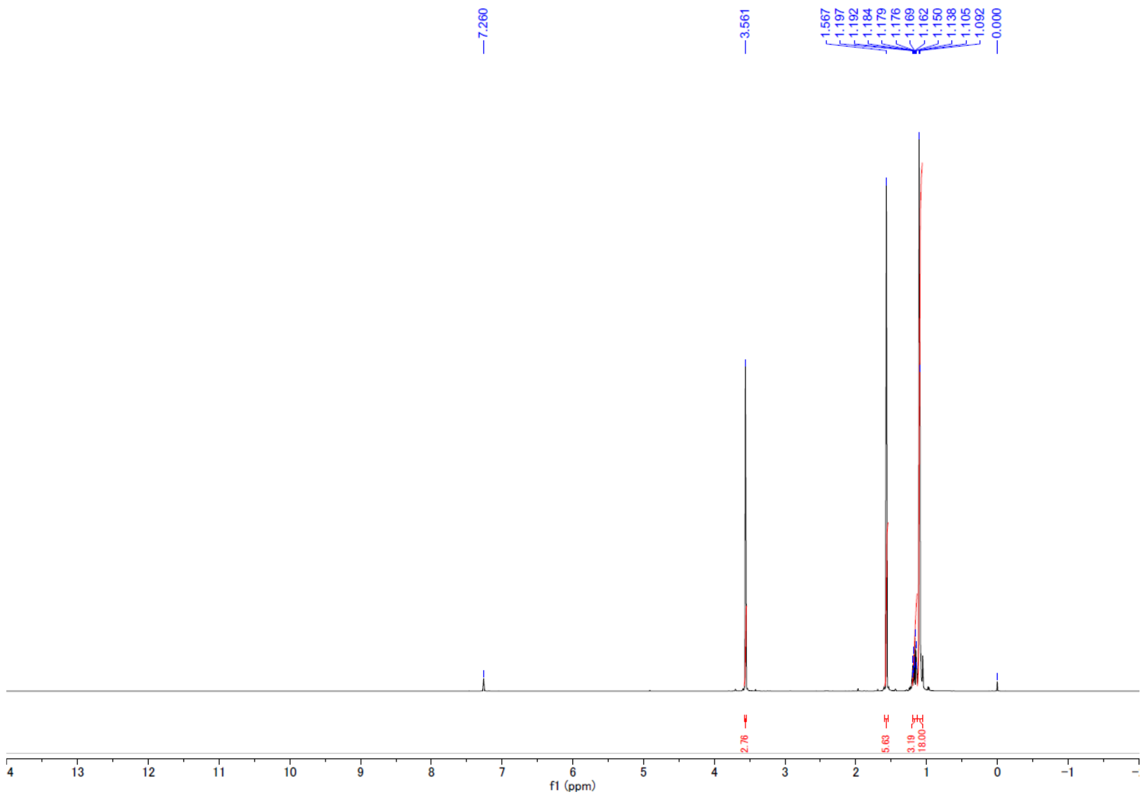

Figure S10. ^{1}H NMR spectrum of ^{iPr3}SKA in $CDCl_3$ at room temperature.

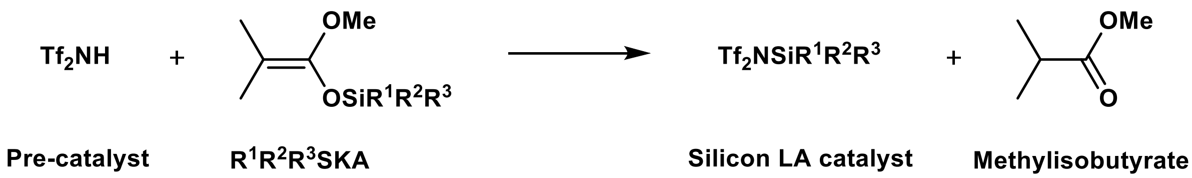

Scheme S1. Generation of a silicon LA catalyst in situ.

Table S1. Summarized data on the GTP of EC using silicon LA catalysts and SKAs having various trialkylsilyl moieties[a]

Entry	^{R1R2R3}SKA	$Tf_2NSiR^1R^2R^3$	Temperature	$[EC]_0$	$[^{R1R2R3}SKA]_0$	$[Tf_2NSiR^1R^2R^3]_0$	Time	Conv. [b]	M_n [c]	$Đ$ [c]
			°C	M	M	M	h	%	g mol^{-1}	M_w/M_n
1	^{Et3}SKA	Tf_2NSiEt_3	10	2.0	0.0050	0.0050	2	25.6	25,300	1.12
2							4	46.8	46,000	1.09
3							8	72.7	66,500	1.18
4							16	72.6	67,600	1.18
5				1.5	0.0050	0.0050	2	36.8	30,000	1.09
6							4	63.6	50,800	1.10
7							8	76.4	60,900	1.18
8							16	78.0	61,300	1.25
9				2.0	0.0050	0.0025	4	27.0	25,200	1.12
10							8	47.6	45,900	1.10
11							24	72.5	65,400	1.18
12							48	71.5	66,000	1.18
13				1.0	0.0025	0.0025	2	16.1	17,100	1.18
14							4	27.4	32,700	1.10
15							12	47.8	54,200	1.20
16							24	47.9	53,500	1.19
17			−40	2.0	0.0050	0.0050	8	7.8	6,800	1.31
18							24	20.0	20,400	1.20
19							72	53.0	56,300	1.13
20							168	100.0	99,800	1.23
21			−30	2.0	0.0050	0.0050	8	14.1	12,900	1.23
22							24	37.5	39,300	1.10
23							72	96.7	90,500	1.19
24							168	100.0	91,100	1.20
25			−20	2.0	0.0050	0.0050	8	23.8	23,600	1.14
26							24	68.6	64,800	1.10
27							48	100.0	94,200	1.19
28							72	100.0	93,800	1.20

29			−10	2.0	0.0050	0.0050	4	20.8	20,500	1.16
30							8	41.2	40,800	1.08
31							24	99.4	87,800	1.18
32							48	100.0	87,200	1.17
33			30	2.0	0.0050	0.0050	1	24.0	25,200	1.13
34							2	38.3	42,600	1.12
35							4	47.1	50,300	1.18
36							8	46.2	50,300	1.19
37	$^{t\mathrm{BuMe2}}$SKA	$\mathrm{Tf_2NSi^{\mathit{t}}BuMe_2}$	30	2.0	0.0050	0.0050	1	23.0	22,300	1.15
38							2	41.8	39,800	1.17
39							4	70.9	66,100	1.16
40							8	88.6	79,500	1.25
41							16	89.3	79,800	1.23
42							24	88.9	84,700	1.23
43				1.5	0.0050	0.0050	1	34.0	26,000	1.11
44							2	63.4	46,800	1.10
45							4	95.9	57,500	1.21
46							8	96.1	60,800	1.18
47				2.0	0.0050	0.0025	2	23.9	21,800	1.21
48							4	44.7	39,400	1.12
49							8	73.5	62,700	1.17
50							16	86.0	71,600	1.24
51				1.0	0.0025	0.0025	4	47.8	50,900	1.09
52							8	65.2	69,800	1.15
53							16	67.2	62,500	1.24
54							24	65.0	60,800	1.25
55			0	2.0	0.0050	0.0050	8	39.3	40,000	1.20
56							16	69.0	70,600	1.23
57							24	100.0	72,700	1.39
58							48	100.0	82,500	1.39
59			15	2.0	0.0050	0.0050	3	36.1	35,500	1.13
60							6	67.3	61,800	1.15

61							12	100.0	85,700	1.23
62							24	100.0	78,400	1.23
63			37.5	2.0	0.0050	0.0050	1	27.8	22,700	1.35
64							2	48.4	47,400	1.13
65							4	70.7	66,900	1.20
66							8	72.0	64,700	1.22
67	^{iPr3}SKA	$Tf_2NSi^iPr_3$	40	2.0	0.0050	0.0050	2	15.0	13,200	1.25
68							4	26.1	23,300	1.21
69							8	43.9	37,800	1.20
70							16	72.6	57,200	1.20
71							24	86.2	63,800	1.24
72							48	97.6	67,500	1.29
73							96	100.0	69,900	1.24
74				1.5	0.0050	0.0050	4	42.8	29,400	1.15
75							8	78.2	50,800	1.13
76							24	100.0	59,800	1.15
77							48	100.0	59,200	1.16
78				2.0	0.0050	0.0025	8	25.8	22,800	1.21
79							24	52.8	45,700	1.14
80							48	69.1	53,700	1.18
81							96	85.2	60,300	1.21
82				1.0	0.0025	0.0025	8	34.6	31,700	1.17
83							24	71.2	57,100	1.19
84							48	87.7	64,500	1.25
85							72	83.8	61,300	1.26
86			30	2.0	0.0050	0.0050	4	19.3	18,300	1.23
87							8	34.7	34,400	1.16
88							24	97.9	78,700	1.20
89							48	100.0	80,800	1.21
90							72	100.0	81,400	1.19
91							120	100.0	80,600	1.21
92			50	2.0	0.0050	0.0050	2	17.5	15,100	1.26

93						4	27.0	22,600	1.26
94						8	36.7	28,500	1.29
95						16	41.4	30,400	1.31
96						24	43.1	30,400	1.35
97						48	44.4	31,700	1.32
98		60	2.0	0.0050	0.0050	1	11.3	9,100	1.25
99						2	14.8	12,000	1.29
100						4	17.7	12,800	1.37
101						8	17.6	13,500	1.36
102						16	17.8	12,800	1.35

[a] Performed on an aluminum block in an argon atmosphere. The silicon LA catalyst was generated via the reaction of ^{R1R2R3}SKA and Tf_2NTH in situ. CH_2Cl_2 was used as the reaction solvent for entries 1–66; 1,2-dichloroethane was used as the reaction solvent for entries 67–102.

[b] Monomer conversion was calculated from the sum of weights of hexane-insoluble and hexane-soluble parts.

[c] Number-averaged molecular weight (M_n) and dispersity ($Đ$) were determined using conventional GPC against PSt standards in $CHCl_3$. Small high-molecular-weight peaks (>10^6 g/mol), attributable to polymer aggregation, were present in the case of entries 39–42, 45, 46, 48–50, 53, 54, and 88–91 (<5%); in the case of entries 60–62 (<20%); and in the case of entries 55–58 (<30%).